Effects of Reactive Compatibilization on the Morphological, Thermal, Mechanical, and Rheological Properties of Intumescent Flame-Retardant Polypropylene

Pingan Song,[†,‡] Yu Shen,[†,‡] Baoxian Du,[†,‡] Mao Peng,[†] Lie Shen,[†] and Zhengping Fang*,[†,‡]

Institute of Polymer Composites, MOE Key Laboratory of Macromolecular Synthesis and Functionalization, Zhejiang University, Hangzhou 310027, China, and Laboratory of Polymer Materials and Engineering, Ningbo Institute of Technology, Zhejiang University, Ningbo 315100, People's Republic of China

ABSTRACT Flame-retardant polypropylene (PP) samples were in situ compatibilized with maleic anhydride grafted PP. Compatibilization reaction was verified by an IR spectrum and gel content measurements. Electron microscopy images showed that compatibilization could considerably reduce the size of the flame-retardant domains, control the phase morphology, and improve the interfacial adhesion between PP and intumescent flame retardant (IFR) with different IFR loading levels. The limiting oxygen index (LOI) of flame-retardant PP increased to different extents after compatibilization, indicating an improvement in the flame retardancy. Compatibilization enhanced the thermal stability to some extent and remarkably delayed thermal oxidative degradation of flame-retardant PP. For PP containing 20 wt % flame retardant, the temperature at which the maximum weight loss rate occurred was enhanced by about 99 °C after compatibilization. The storage modulus and glass transition temperatures were elevated to different extents. Tensile strengths of samples reduced in the presence of flame retardant alone but in the additional presence of compatibilizer were restored to levels similar to those of pure PP. Elongation-at-break values, however, showed IFR concentration-dependent reductions that were less for compatibilized samples. Furthermore, the complex viscosity of a compatibilized PP melt turned slightly smaller, which is favorable to melt processing.

KEYWORDS: reactive compatibilization • polypropylene • morphology • thermal properties • mechanical property • rheological properties

INTRODUCTION

Polypropylene (PP) is a widely used thermoplastic material in lots of fields because of its easy processing property, low density, excellent mechanical properties, and so on (1, 2). However, the inherent flammability of PP, with a limiting oxygen index (LOI) typically of 17.4, limits its application in some fields like electronic appliances where high flame retardancy is required. In the past decades, intumescent flame retardants (IFRs) are found to be effective flame retardants for thermoplastic resins like PP and polyethylene (PE) (3−7). Typically, 25−30% by mass IFR is needed to make PP or PE achieve the ideal flame retardancy, which means that the flame-retardant formulations could pass two fire test methods commonly used, LOI and UL-94 (8, 9). Generally, when achieving both LOI ≥ 28 and a V-0 rating, the flame-retardant materials are considered to have rather excellent flame retardancy and could almost be used in various fields.

When excellent flame retardancy is conferred on polymeric materials, flame retardants (IFRs) may reduce the mechanical properties and other properties of the materials and simultaneously may also worsen the processing conditions because the rather different polarities of IFRs and PP make them thermodynamically immiscible (10). Meanwhile, the differences in polarity cause a weak interfacial adhesion, which plays an important role in the mechanical and other related properties. Therefore, on the one hand, the mechanical properties like the tensile strength and impact strength of the flame-retardant polymeric materials may not reach the standards required practically; on the other hand, their processing conditions may turn much sterner, which will create many difficulties during processing.

Reactive compatibilization (11−16) has been proven to be an effective method for improving the interfacial adhesion and morphology control in a variety of incompatible blends. The reactive interfacial agents with special functional groups are able to generate in situ formation of block or graft copolymers at the interface during the compounding process. Moreover, new chemical bonds created during blend fabrication have much stronger interactions than weaker physical interaction forces like hydrogen bonds and van der Waals forces (12−14).

However, the fundamental understanding of reactive compatibilization on flame-retardant polymeric composites

Scheme 1. Schematic Representation for Possible Compatibilization Reaction between PPMA and Flame-Retardant PDBPP
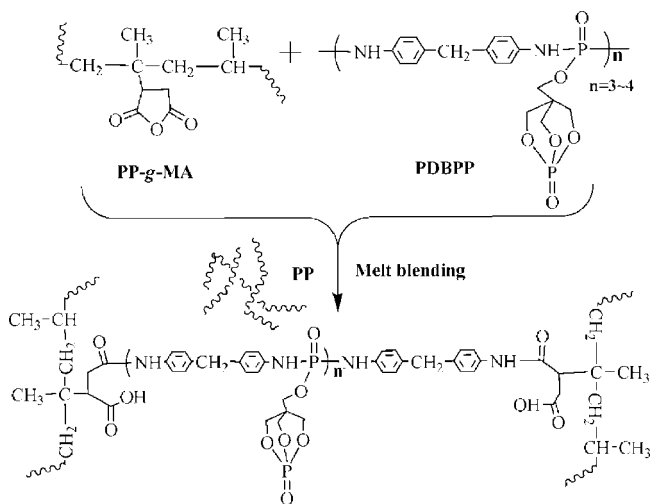
Table 1. Formulations of Flame-Retardant PP and Corresponding Compatibilized PP Systems, as Well as Their LOI Values

sample ID	PP	PPMA	PDBPP	LOI (%)
PP	100	0	0	17.4
PP/10% PDBPP	90	0	10	21.5
PP/20% PDBPP	80	0	20	25.0
PP/30% PDBPP	70	0	30	28.0
C-PP/10% PDBPP	85	5	10	22.6
C-PP/20% PDBPP	70	10	20	26.5
C-PP/30% PDBPP	55	15	30	29.4
PP/5% PPMA	95	5	0	17.4
PP/10% PPMA	90	10	0	17.4
PP/15% PPMA	85	15	0	17.3

is relatively limited. In our previous work (17, 18), we synthesized a novel oligomeric IFR, poly(4,4-diaminodiphenylmethane-*O*-bicyclic pentaerythritol phosphate phosphate) (PDBPP; see Scheme 1), which was able to endow good flame retardancy on PP, while the morphological, mechanical, and rheological properties of the flame-retardant systems remain to be further investigated. In this study, on the basis of PDBPP comprising active bifunctional groups (NH₂ or NH), we use maleic anhydride grafted PP (PPMA) as the compatibilizer and consider the effects of reactive compatibilization on the morphological, thermal, mechanical, and rheological properties of the flame-retardant systems.

EXPERIMENTAL SECTION

Materials. Polypropylene (PP; M_n = 270 000, MFR = 3.0 g/min) was purchased from Shanghai Petrochemicals Factory, and maleic anhydride grafted PP (PPMA; MA content = 1 wt %) was obtained from Shanghai Rizhisheng Ltd. Co. The flame retardant, PDBPP, was synthesized according to the procedure in the literature (17, 18).

Fabrication of Samples. The composites were fabricated via melt compounding of PP, PPMA, and PDBPP according to the formulations presented in Table 1 at 180 °C in a ThermoHaake Rheomix compounder with a rotor speed of 60 rpm and a mixing time of 8 min for each sample. The samples prepared were transferred to a mold, preheated for 5 min at 180 °C, and pressed at 15 MPa followed by cooling to room temperature while maintaining the same pressure for 5 min. The sample sheets obtained were stored for further tests.

IR Spectroscopy. IR measurements were performed on a Vector-22 FT-IR spectrometer using KBr pellets for PDBPP and a film-pressing method for PP/PPMA and C-PP/30% PDBPP samples, respectively.

Gel Content Measurements. The gel content (wt %) of the sample was obtained using a Soxhlet extractor by refluxing PP, PP/PPMA, and PP/PDBPP samples in boiling xylene at 135 °C for 48 h. As for PP/PDBPP samples, their gel contents were the values that were deducted from the PDBPP content in flame-retardant PP samples.

Morphological Characterization. Scanning electron microscopy (SEM) images were recorded on a SIRION-100 (FEI, Hillsboro, OR) scanning electron microscope at an accelerating voltage of 10 kV. Transmission electron microscopy (TEM) measurements were conducted on a JEM-1200EX transmission electron microscope.

If the particles were large enough for accurate analysis, different micrographs with a total amount of over 200 particles were chosen. These micrographs were analyzed with the aid of image analysis software, and the diameter of each particle was measured. A number-average diameter (D_n) was calculated according to the following formula (1).

$$D_n = \sum N_i D_i / \sum N_i \tag{1}$$

Thermogravimetric Analysis (TGA). TGA was performed on a TA SDTQ600 thermal analyzer at a scanning rate of 20 °C/min both in nitrogen and in air. The measurement temperature range was from room temperature to 600 °C. The TGA tests were done in triplicate for each sample. The reproducibilities of temperature and mass were ±1 °C and ±0.1 wt %.

Tensile Measurements. Tensile properties of samples were measured with a WD-5 Electric Tensile Tester at 25 ± 2 °C, and the data reported here were the means of quintuplicate experiments.

Dynamic Mechanical Analysis (DMA). DMA was performed on a DMA242C dynamic mechanical analyzer. A temperature range from −50 to 150 °C at a heating rate of 3 °C/min and a frequency of 2 Hz was used after optimization of the static and dynamic loads.

Rheological Analysis. Rheological properties were evaluated using an advanced rheological expanded system with parallel-plate geometry of 25 mm in diameter. The storage modulus (G'), loss modulus (G''), and complex viscosity (η^*) were measured in the frequency sweep experiments performed at 180 °C over a frequency range of 0.01−100 rad/s, with data collected at five points per decade. The strain γ was controlled at 1 % during the measurements.

RESULTS AND DISCUSSION

Compatibilization Mechanism. Take the fact that flame-retardant PDBPP possesses active end-functional groups (NH₂ or NH), which can react with the maleic anhydride groups in PPMA to generate graft copolymers during blend fabrication. The graft products can serve as compatibilizers and compatibilize the PP/PDBPP system. The possible compatibilization reaction is shown in Scheme 1, and the reaction mechanism is similar to our assumption. To verify this reaction, IR and gel content measurements were performed, with IR spectra of (a) PP/15% PPMA, (c) C-PP/30% PDBPP, and (b) flame-retardant PDBPP shown in Figure 1. For flame-retardant PDBPP, the IR spectrum shows
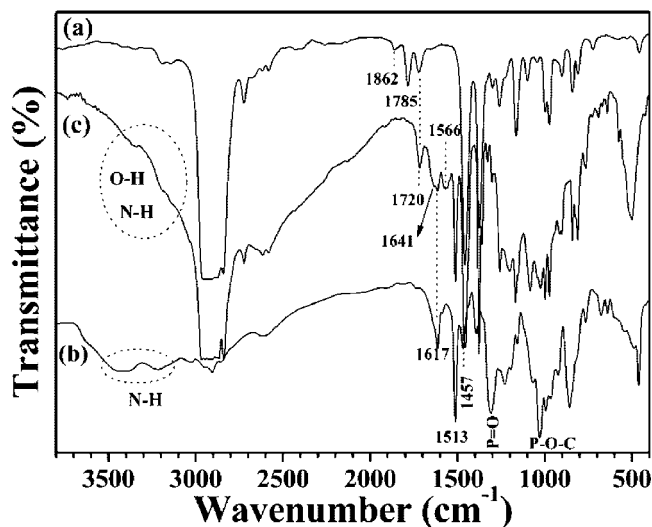
FIGURE 1. IR spectra for (a) PP/15% PPMA, (b) PDBPP, and (c) C-PP/30% PDBPP.

that absorption peaks at 1306 cm^{-1} (vs, P=O), 1025 cm^{-1} (vs, P−O−C), 3440 and 3231 cm^{-1} (vs, N−H), 1624, 1517, and 1457 cm^{-1} (characteristic peaks of phenyl), 1345, 1240, and 960 cm^{-1} (vs, P−N) appear, which confirms the chemical structure of PDBPP (17, 18). For the IR spectrum of the PP/15% PPMA sample, the absorption peak at 1720 cm^{-1} is assigned to carbonyl groups that are due to oxidation of the sample during fabrication and two absorption peaks at 1862 and 1785 cm^{-1} are attributed to asymmetric and symmetric stretching vibrations of carbonyl groups in maleic anhydride groups of PPMA molecules, respectively (19, 20), while for C-PP/30% PDBPP, the two peaks at 1862 and 1785 cm^{-1} basically disappear, and the intensity of the peak at 1720 cm^{-1} increases to some extent. Moreover, two new absorption peaks at 1641 and 1566 cm^{-1} appear, which are due to the bending vibration of amide groups generated in a ring-opening reaction between amine groups in a PDBPP molecule and maleic anhydride groups on PPMA. In addition, the double peaks of amine groups at 3440 and 3231 cm^{-1} turn to single peaks, which belong to the stretching vibrations of N−H and O−H groups created during the compatibilization reaction. These changes obviously confirm the compatibilization reaction. On the other hand, the gel will generate if the compatibilization reaction occurred because the graft copolymers are likely cross-link products and do not dissolve in boiling xylene. The gel contents of PP, PP/PPMA, and flame-retardant samples are shown in Figure 2. For PP and PP/PDBPP samples without compatibilization, no gels appear, while in the case of PP/15% PPMA, about 1.5 wt % insoluble gels generate, which may be caused during the preparation of the PPMA sample by a graft reaction or PP/PPMA samples. For C-PP/PDBPP systems, the gel content increases with increasing PDBPP loading, 10.4, 17.9, and 25.1 wt %, respectively. Apparently, all of PDBPP and PPMA were not cross-linked or reacted, the theoretical gel contents of C-PP/10−30% PDBPP should be 15, 30, and 45 wt %, respectively, which means some flame retardants did not react with PPMA and still exist as inert fillers. On the other hand, the amount of PPMA may
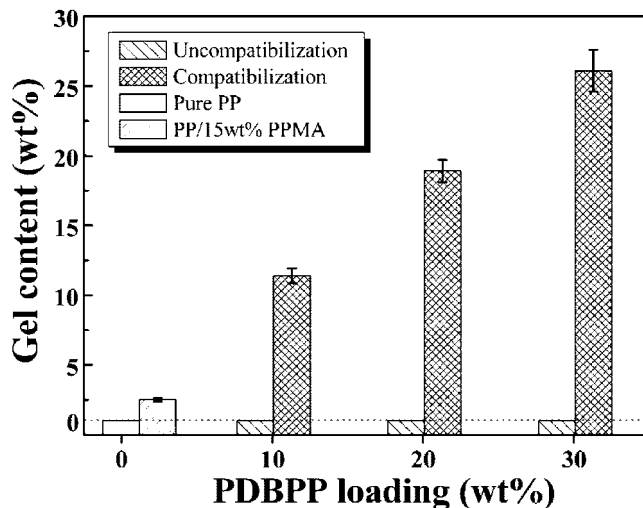

FIGURE 2. Gel contents for PP, PP/15% PPMA, and PP/PDBPP systems before and after compatibilization with PPMA.

not be enough to react with all PDBPP molecules. Despite this, the gel content provides powerful evidence for the compatibilizaiton reaction.

Because the compatibilization reaction occurred, this kind of copolymer not only will reduce the size of the PDBPP particles but also could act as the compatibilizer with a PP matrix, which enabled PDBPP and the matrix to have better interfacial adhesion. Simultaneously, it will also result in changed mechanical and rheological properties, which will be analyzed in the following sections.

Morphology. As expected, the morphology was effectively controlled through the assumptive reactive compatibilization. The SEM and TEM images of fracture sections for PP/PDBPP and statistical diameters of PDBPP particles in the matrix before and after compatibilization are shown in Figure 3 and Figure 4, respectively. Clearly, two important points are readily observed in Figure 3. (1) Before compatibilization, the interfaces between flame-retardant PDBPP and the polymeric matrix are clearly apparent because the images showed many large PDBPP particles or cavities where PDBPP resided as a result of sample fabrication in the matrix. The samples for SEM measurements were fabricated through the cryopreservation−brittle-breaking method because of the interface adhesion force between the matrix and PDBPP; consequently, PDBPP was rather easy to drop, and cavities subsequently formed. (2) After compatibilization with PPMA, for each PP/PDBPP system, almost no obvious interfaces are observed between fillers and the matrix at low magnification; however, the interfaces still can be recognized at higher magnification. TEM images (see Figure 4) show that large flame-retardant domains (marked by black arrows) appear in the PP/20% PDBPP and PP/30% PDBPP samples; some flame retardants dropped from the PDBPP domains during fabrication of samples for TEM tests (marked by white arrows). After compatibilization, a large number of small flame-retardant particles can be observed in C-PP/PDBPP samples; however, some larger PDBPP particles remain but are still smaller than those in the PP/PDBPP samples which is consistent with the results of gel content
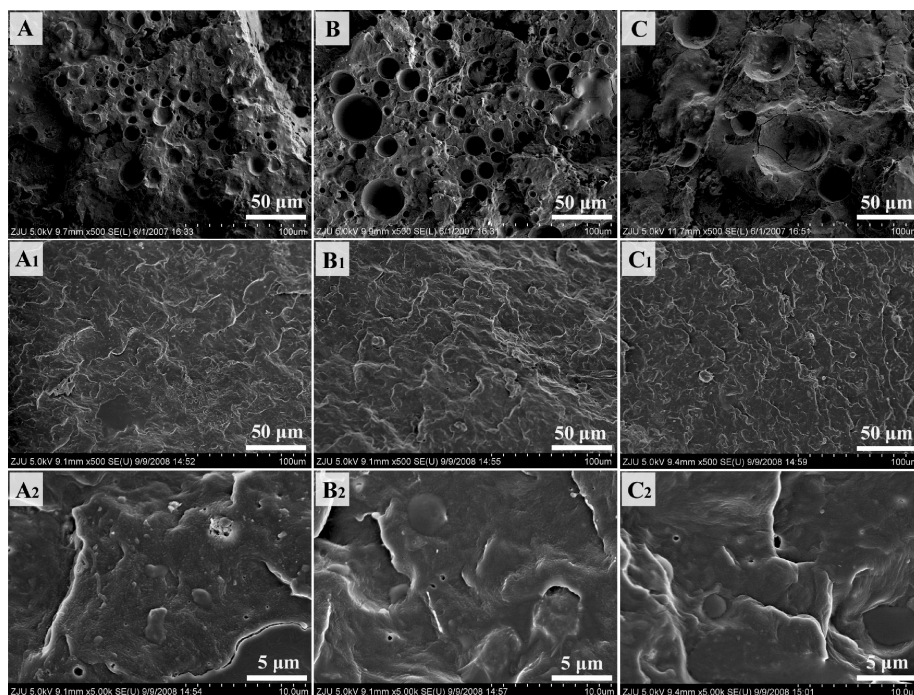
FIGURE 3. SEM images for PP/PDBPP systems before and after compatibilization with PPMA: (A) PP/10% PDBPP, (B) PP/20% PDBPP, (C) PP/30% PDBPP; (A₁, A₂) C-PP/10% PDBPP, (B₁, B₂) C-PP/20% PDBPP, (C₁,C₂) C-PP/30% PDBPP. A₂, B₂, and C₂ are the SEM images of A₁, B₁, and C₁ at higher magnification.
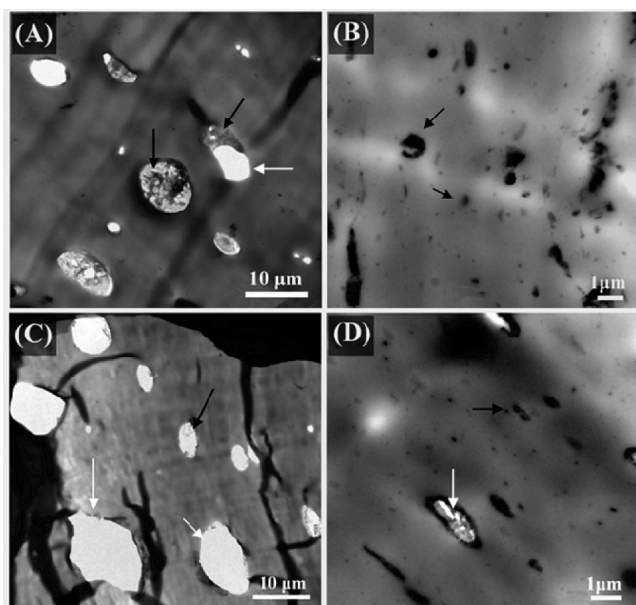

FIGURE 4. TEM images for PP/PDBPP systems before and after compatibilization with PPMA: (A) PP/20% PDBPP, (B) C-PP/20% PDBPP, (C) PP/30% PDBPP, and (D) C-PP/30% PDBPP.

measurements. Statistical data (see Figure 5) obtained from SEM and TEM images showed that number-average diameters of PDBPP domains increased to some extent with increasing PDBPP loading levels, yielding a D_n range of around $4.5 \pm 0.5 - 8.2 \pm 1.5 \mu$m, while after compatibilization, the D_n values varied from around 0.5 ± 0.1 to $0.8 \pm 0.2 \mu$m. The observations and statistical data indicated that the in situ reactive compatibilization was rather effective in terms of reducing the size of the PDBPP domains and improving the interfacial adhesion between PDBPP and the PP matrix.
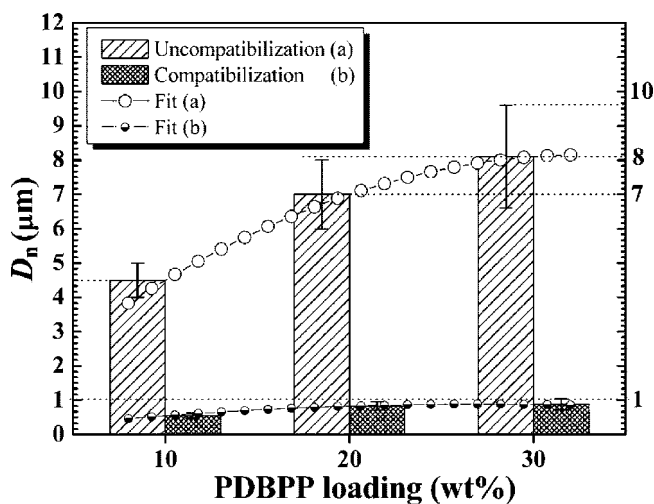

FIGURE 5. Statistical graphs of diameters for PDBPP particles as a function of PDBPP loading before and after compatibilization: (○) fitting line of PP/PDBPP samples without compatibilization; (◖) fitting line of PP/PDBPP samples with compatibilization.

Flame Retardancy. LOI, the minimum oxygen concentration by volume for maintaining the burning of a material, is a very important parameter for evaluating the flame retardancy of a polymeric material. Generally, the higher the LOI value, the better the flame retardancy of the material. Table 1 shows the LOI values for all samples discussed in this research. Obviously, the LOI values of different flame-retardant PP increased to different extents in the range of 0.9–1.5 vol % because better dispersion of PDBPP in the PP matrix made flame-retardant samples more difficult to ignite and consequently needed a higher oxygen concentration to support burning of the samples. Because the incorporation of PPMA did change the LOI value to some
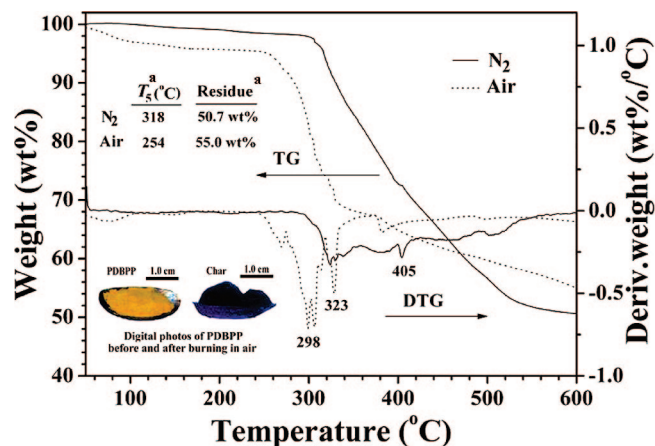
FIGURE 6. TGA and DTG curves of flame-retardant PDBPP in air and nitrogen atmospheres. Footnote *a*: T_5 is the temperature at which 5 wt % weight loss occurred. Residue (wt %) was obtained at 600 °C.
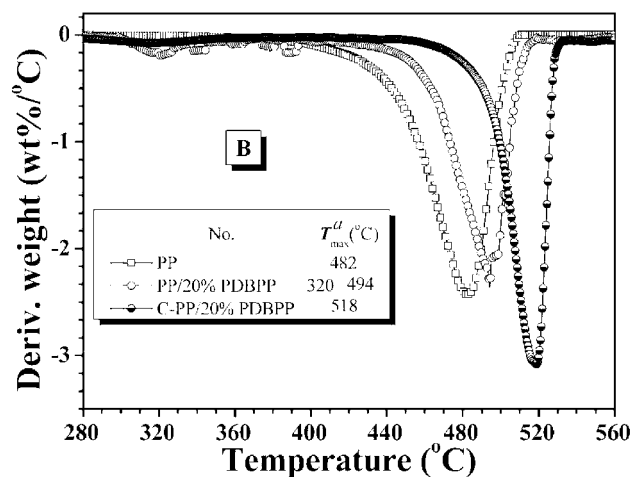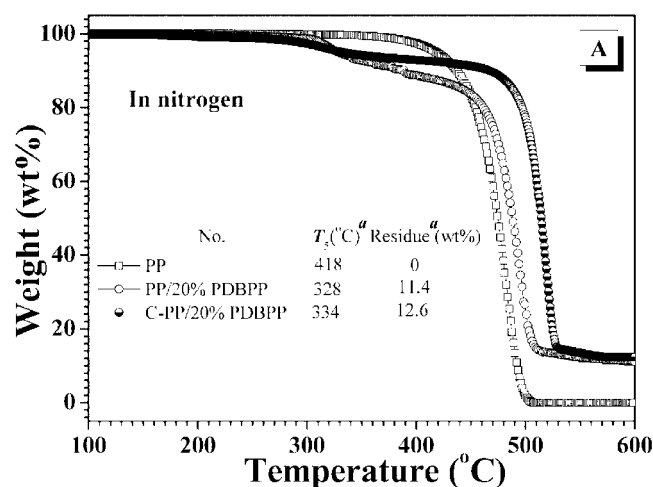

FIGURE 7. (A) TGA and (B) DTG curves of pure PP, PP/20 % PDBPP, and C- PP/20 % PDBPP in nitrogen. Footnote *a*: T_5 and T_{max} are the temperatures at which 5 wt % weight loss and the maximum weight loss rate occurred, respectively. Residue (wt %) was obtained at 600 °C.

extent, reactive compatibilization contributed to the flame retardancy of the samples.

Thermal Stability. Figure 6 shows the TGA and differential thermogravimetry (DTG) curves for flame-retardant
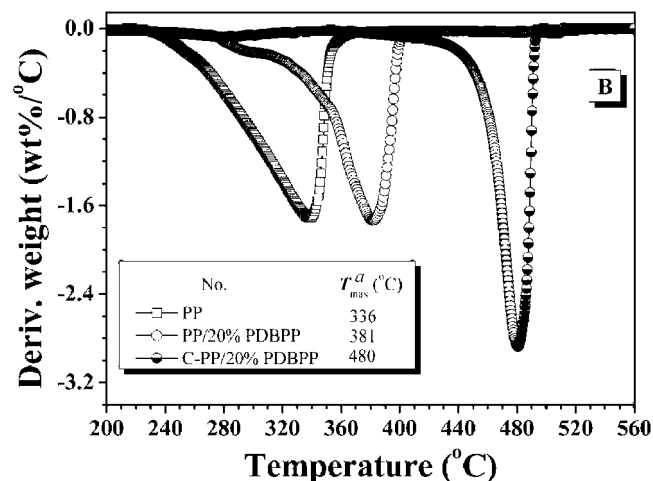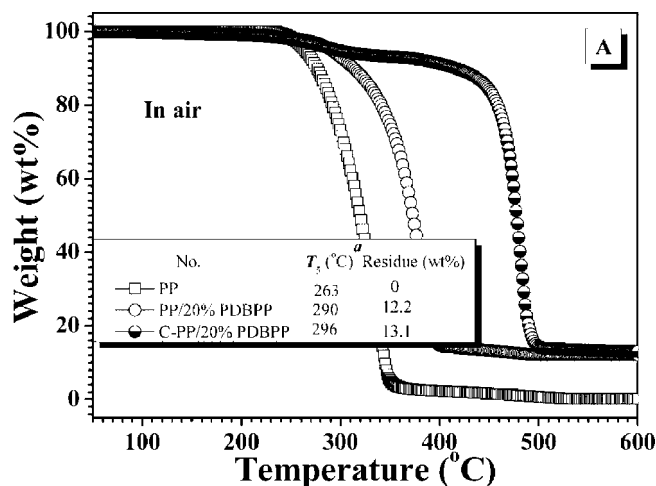

FIGURE 8. (A) TGA and (B) DTG curves of pure PP, PP/20 % PDBPP, and C- PP/20 % PDBPP in air. Footnote *a*: T_5 and T_{max} are the temperatures at which 5 wt % weight loss and the maximum weight loss rate occurred, respectively. Residue (wt %) was obtained at 600 °C.

PDBPP in nitrogen and air atmospheres. PDBPP starts to degrade at 318 °C in nitrogen and at 254 °C in air (the initial degradation temperature is defined as T_5, where 5 wt % mass loss takes place in our laboratory). The maximum weight loss temperature of PDBPP is similar to T_5, but the degradation mode is more complex in air than in nitrogen. The char residues of PDBPP at 600 °C are 50.7 wt % in nitrogen and 55.0 wt % in air; the higher residue of the latter is due to the oxidation reaction, and the high residue suggests that PDBPP is an excellent char-forming agent. Figure 6 also gives a digital photograph of PDBPP before and after burning in air, which suggests PDBPP is an IFR.

Because PP was flame retardant with PDBPP, the data obtained from TGA are very important because TGA could give some useful information about thermal stability and thermal oxidation degradation of flame-retardant PP. Here, we only give typical TGA results for PP/20 % PDBPP with and without compatibilization as a comparison because the other two samples possess similar results. The TGA and DTG curves and derivative information from the curves in nitrogen and air are presented in Figures 7 and 8, respectively. The temperature at which 5 wt % weight loss occurred (T_5;
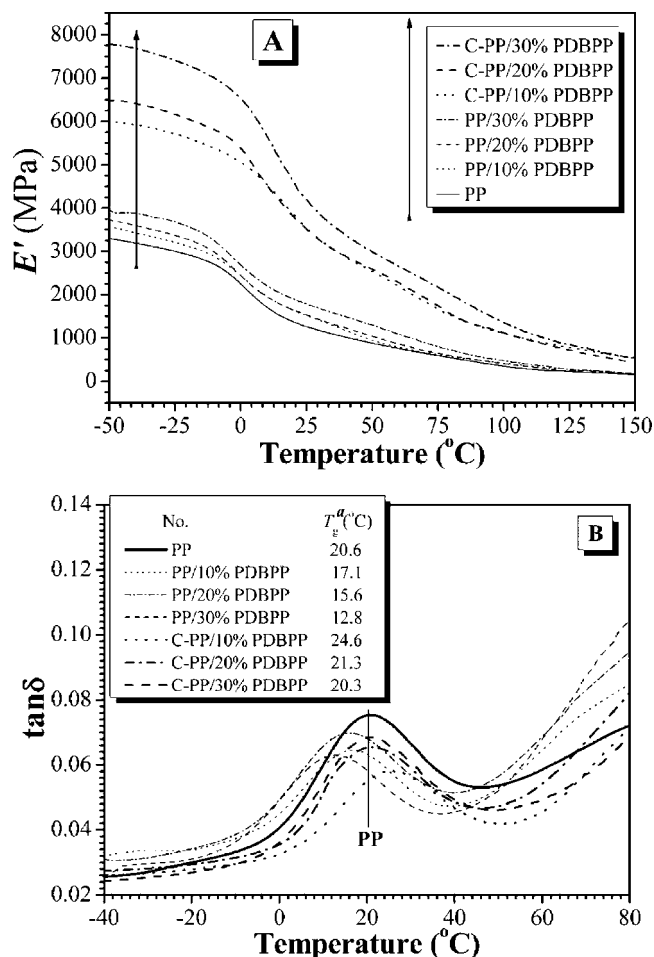
FIGURE 9. DMA curves of PP, PP/PDBPP, and C- PP/PDBPP systems: (A) storage modulus vs temperature; (B) loss factor vs temperature. Footnote *a*: T_g values were obtained from the peak values in the loss factor (tan δ) vs temperature.

FIGURE 10. Tensile measurements of PP, PP/PDBPP, and C-PP/PDBPP systems: (A) tensile stress and (B) elongation at break vs PDBPP content.

often considered to be the initial degradation temperature) and the temperature at which the maximum weight loss rate occurred (T_{max}) are two important parameters that can reflect the thermal stability of the material. In nitrogen, PP alone started to degrade at about 418 °C and the maximum weight loss rate occurred at about 482 °C, leaving no residue char at 600 °C. After incorporation of 20 wt % PDBPP into PP, the initial degradation temperature happened at 328 °C, which was due to decomposition of PDBPP, and T_{max} was delayed up to 494 °C, about 12 °C higher than that of PP, with a residue of 11.4 wt % left. It should be noted that the smaller maximum at $T_{max} = 320$ °C was also attributed to the decomposition of PDBPP. These temperature changes demonstrated that PDBPP could enhance the thermal stability of PP to some degree, while after compatibilization, both T_5 and T_{max} were further enhanced to different extents, about 6 and 24 °C, respectively. In addition, the residue also increased up to 12.6 wt % probably because of the cross-linking reaction between PDBPP and PPMA, which was equally important for improving the thermal stability of PP. On the basis of the above discussion, we can easily see that reactive compatibilization could enhance the thermal stability of flame-retardant PP.
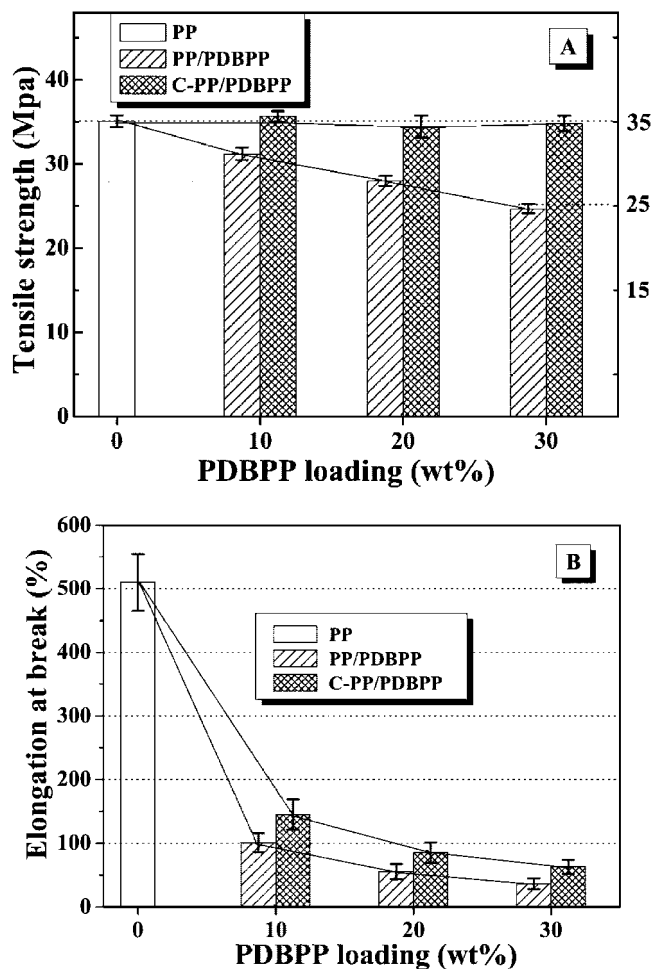
In an air atmosphere, the thermal oxidation degradation is of primary importance, which can determine the antithermal oxidative stability of a polymer and is considered to be much more important for relating to the processing and service-life performance of certain flame-retardant formulations. PP started to decompose at 263 °C and T_{max} took place at about 336 °C, still leaving no residue at 600 °C. After introduction of PDBPP into the PP matrix, the T_5 and T_{max} values were delayed up to 290 and 381 °C, respectively, and the residue increased to 12.2 wt %. After compatibilization, T_5 and T_{max} were further (and mainly for T_{max}) enhanced up to 296 and 480 °C, about 6 and 99 °C higher than those before compatibilization. Moreover, the residue increased up to 13.1 wt %. Both temperature changes and residue char indicated that compatibilization could considerably delay thermal oxidation degradation of flame-retardant PP. These surprising results are of possibly great significance for a flame-retardant material performance generally.

Dynamic Mechanical Behavior. Figure 9 presented the graphs for the (A) storage modulus and (B) loss factor versus the temperature of PP and its flame-retardant formulations before and after compatibilization. Before compatibilization, we could readily observe that the storage modulus (E') monotonously increased with an increase in
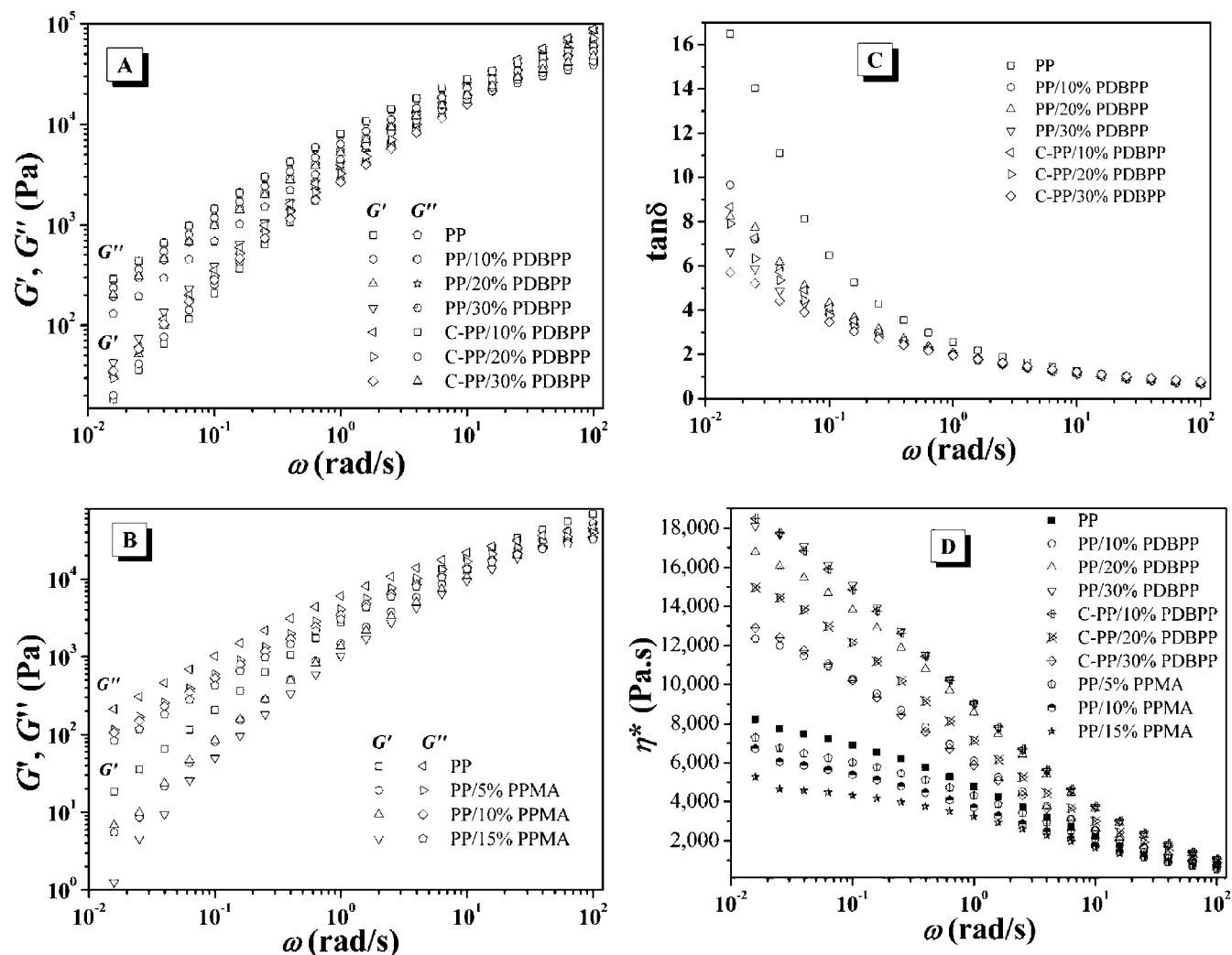
FIGURE 11. (A) G' and G'' vs ω for PP, PP/PDBPP, and C-PP/PDBPP systems, (B) G' and G'' vs ω for PP and PP/PPMA systems, (C) tan δ vs ω for PP, PP/PDBPP, and C-PP/PDBPP systems, and (D) η^* vs ω for PP, PP/PDBPP, and C-PP/PDBPP as well as PP/PPMA systems.

the PDBPP content over the temperature range, which was attributed to the reinforcement effects of fillers. Unexpectedly, the glass transition temperature (T_g) gradually shifted to lower temperature with increasing PDBPP loading levels; a T_g value decreases from 20.6 °C for PP and 12.8 °C for PP/30 % PDBPP. This may be due to the plasticization effects also caused by the flame retardant. After reactive compatibilization, the storage modulus considerably increased, effectively doubling that for the corresponding flame-retardant PP without compatibilizer. Furthermore, unlike those with uncompatibilized PP, the T_g values of compatibilized PP shifted to higher temperature. However, with an increase in the PDBPP content, T_g returned to a lower temperature again but was still higher than that of pure PP except for PP/30 % PDBPP, which was also attributed to the plasticization effects of PDBPP because a few large PDBPP particles still existed after compatibilization. Both significant changes were attributed the in situ reactive compatibilization reaction, which formed many physical or chemical cross-linkage sites and limited the free movement of chain segments. Consequently, further increases in the storage modulus occurred and the T_g values shifted to higher temperature.

On the basis of the results obtained from dynamic mechanical analysis, we can obviously see that the reactive compatibilization not only significantly enhanced thermal properties but also remarkably improved the dynamic mechanical properties of immiscible composites.

Tensile Properties. Because in situ compatibilization reaction considerably elevated the dynamic mechanical properties, it may also be considered to improve the tensile strength to some extent. Figure 10 shows the tensile strength (A) and elongation at break (B) plots versus PDBPP content before and after compatibilization. Before compatibilization, both the tensile strength and elongation at break gradually decreased to different extents with increasing PDBPP content, for example, a tensile strength value of 35.1 MPa and around 510 % of the elongation at break for PP, while being 25 MPa and 46 %, respectively, for PP/30 % PDBPP. However, after compatibilization, the tensile strengths were basically the same as that of pure PP, although the elongation-at-break values were only slightly improved compared with uncompatibilized samples. These surprising results are of significance for flame-retardant PP composites and mean that compatibilized flame-retardant composites

ACS APPLIED MATERIALS & INTERFACES Song et al. www.acsami.org

could basically meet expected tensile strength requirements during application.

Rheological Properies. Studies on the rheological behavior of a polymeric material may contribute to the fundamental understanding of the practical processing efficiency, and so from a practical application view, they are of great importance. Figure 11 showed the plots of (A) G' and G'' vs ω, (C) loss factor (tan δ) vs ω, and (D) complex viscosity (η^*) vs ω for PP and PP/PDBPP composites before and after compatibilization and (B) G' and G'' vs ω for PP and PP/PPMA systems as a comparison. It was not difficult to observe that all values of the storage modulus, loss modulus, and complex viscosity of the flame-retardant PP samples were much higher than those of PP alone over the whole frequency range, which is further evidence for the reinforcement effects of fillers and the simultaneous effects on the rheological behavior. However, these three parameters were slightly smaller after compatibilization than those before compatibilization, which means that in situ compatibilization seems to make the processing of the materials easier because of the smaller melt viscosity. To clarify the reason for this behavior, we employed PP systems containing the same concentration of the compatibilizer PPMA (see Figure 11B) as a comparison, and both the storage and loss moduli were obviously much lower than those of pure PP, which was due to the dilution effect of the lower molecular weight PPMA over the whole frequency range. In addition, the loss factors of all flame-retardant PP were lower than those of PP and, furthermore, tan δ gradually decreased with increasing PDBPP contents both before and after compatibilization. Through analysis of the rheological behavior of the composites, we could draw one simple conclusion that while in situ compatibilization did not markedly change the rheological behavior of the composites, it could make the processing of composites slightly easier.

CONCLUSIONS

PPMA was employed as the compatibilizer for flame-retardant PP systems, in which maleic anhydride groups could react with functional groups (NH) present on the flame-retardant monomer to form in situ graft copolymer, whose chemical structure was verified. This compatibilization significantly reduced the size of the dispersed PDBPP phase domains and improved the interfacial adhesion of PP and flame-retardant PDBPP; thus, expected compatibilization effects were achieved. Furthermore, compatibilization enhanced the thermal stability and considerably delayed the thermal oxidation degradation of PP. The mechanical properties were remarkably improved after compatibilization because tensile strengths attained values similar to that of pure PP even when 30 wt % PDBPP was present. In addition, storage modulus values were about twice those of composites without compatibilization. Moreover, in situ compatibilization reduced the melt viscosity of the flame-retardant PP, thus making processing much easier.

REFERENCES AND NOTES

(1) Uotila, R.; Hippi, U.; Paavola, S.; Seppälä, J. *Polymer* **2005**, *46*, 7923.
(2) Li, Q.; Jiang, P. K.; Su, Z. P.; Wei, P.; Wang, G. L.; Tang, X. Z. *J. Appl. Polym. Sci.* **2005**, *96*, 854.
(3) Wu, Q.; Qiu, B. J. *Polym. Degrad. Stab.* **2001**, *74*, 255.
(4) Lv, P.; Wang, Z. Z.; Hu, K. L.; Fan, W. C. *Polym. Degrad. Stab.* **2005**, *90*, 523.
(5) Li, B.; Xu, M. J. *Polym. Degrad. Stab.* **2006**, *91*, 1380.
(6) Chen, Y. H.; Wang, Q. *Polym. Degrad. Stab.* **2007**, *92*, 280.
(7) Tang, Y.; Hu, Y.; Song, L.; Zong, R. W.; Gui, Z.; Fan, W. C. *Polym. Degrad. Stab.* **2006**, *91*, 234.
(8) Wang, X. Y.; Li, Y.; Liao, W. W.; Gu, J.; Li, D. *Polym. Adv. Technol.* **2008**, *19*, 1055.
(9) Zhou, S.; Wang, Z. Z.; Gui, Z.; Hu, Y. *Fire Mater.* **2008**, *32*, 307.
(10) Shi, D.; Ke, Z.; Yang, J. H.; Gao, Y.; Wu, J.; Yin, J. H. *Macromolecules* **2002**, *35*, 8005.
(11) Dedecker, K.; Groeninckx, G. *Macromolecules* **1999**, *32*, 2472.
(12) Asthana, H.; Jayaraman, K. *Macromolecules* **1999**, *32*, 3412.
(13) Cho, K.; Li, F. K. *Macromolecules* **1998**, *31*, 7495.
(14) Cigana, P.; Favis, B. D.; Albert, C.; Vu-Khanh, T. *Macromolecules* **1997**, *30*, 4163.
(15) Shang, X. Y.; Zhu, Z. K.; Yin, J.; Ma, X. D. *Chem. Mater.* **2002**, *14*, 71.
(16) Zhang, J. F.; Sun, X. Z. *Biomacromolecules* **2004**, *5*, 1446.
(17) Song, P. A.; Fang, Z. P.; Tong, L. F.; Jin, Y. M.; Lu, F. Z. *J. Anal. Appl. Pyrolysis* **2008**, *110*, 616.
(18) Song P. A.; Fang Z. P.; Tong L. F.; Xu Z. B. *Polym. Eng. Sci.* **2009**, in press.
(19) Galia, A.; Grego, R. D.; Spadaro, G.; Scialdone, O.; Filardo, G. *Macromolecules* **2004**, *37*, 4580.
(20) Hayes, H. J.; Han, B.; McCarthy, T. J. *Macromolecules* **1998**, *31*, 4813.

AM8001204